

# Assembling and Disassembling Ag Clusters on Si(111)-(7×7) by Vertical Atomic Manipulation

Fangfei Ming,<sup>†</sup> Kedong Wang,<sup>†</sup> Shuan Pan,<sup>†</sup> Jiepeng Liu,<sup>†</sup> Xieqiu Zhang,<sup>†</sup> Jinlong Yang,<sup>‡</sup> and Xudong Xiao<sup>†,\*</sup>

<sup>†</sup>Department of Physics, The Chinese University of Hong Kong, Shatin, New Territory, Hong Kong, China, and <sup>‡</sup>Hefei National Laboratory for Physical Sciences at Microscales, University of Science and Technology of China, Hefei, Anhui 230026, China

**M**etal clusters possess many unique physical and chemical properties and have attracted extensive studies during the past two decades. The size and the structure of the clusters, either in the free-standing form or in the supported form, often dictate their properties. For example: Na clusters in gas phase reveal a strong size-dependent melting temperature;<sup>1,2</sup> Nb clusters show size-dependent ferroelectricity;<sup>3</sup> supported Au clusters (~2 nm size) have unique low temperature catalytic activity for CO oxidation that depends both on size and shape of the clusters,<sup>4–6</sup> and Al cluster anions demonstrate strong size-selective reactivity with water to produce hydrogen.<sup>7</sup> The size of clusters in gas phase can easily be measured by mass spectroscopy, and their structures have been studied by photoelectron spectroscopy<sup>8</sup> and by far-infrared multiple-photon dissociation (FIR-MPD) spectroscopy.<sup>9</sup> In contrast, the detailed information on the size and structure of supported clusters on surfaces can be obtained only through imaging. Neither transmission electron microscopy<sup>5</sup> nor scanning tunneling microscopy (STM)<sup>6</sup> provides the precision to a single atom because of the limited spatial corrugation of the clusters. We demonstrate here that the surface-supported cluster size can indeed be determined by atomic manipulation to the precision of a single atom. With STM imaging, certain structural information can also be obtained, which can no doubt provide valuable information for the final determination of the structure when first-principles simulation is applied.

Atomic manipulation has been used to construct many nanostructures in the past with high controllability.<sup>10,11</sup> Since the first demonstration of controllable atomic manipulation in 1990,<sup>10</sup> a number of modes have been developed to manipulate single atoms and molecules with atomic precision by using STM and atomic force microscopy

**ABSTRACT** Atomic manipulation has been rarely used in the studies of complex structures and a low temperature requirement usually limits its application. Herein we have demonstrated a vertical manipulation technique to reproducibly and reversibly manipulating Ag atoms on an Si(111)-(7×7) surface by a scanning tunneling microscope tip at room temperature. Simple and complex Ag nanoclusters were assembled and disassembled with a precise control of single Ag atoms, which provided critical information on the size of these nanoclusters. The manipulation showed the growth processes of these Ag clusters and even partly unveiled their atomic structures. This technique can form a fundamental basis for further studies of the Ag/Si(111)-(7×7) system and for fabricating functional nanodevices in various metal–semiconductor systems.

**KEYWORDS:** scanning tunneling microscopy · Si(111)-(7×7) · vertical manipulation · metal on semiconductor · nanocluster

(AFM).<sup>12–15</sup> The majority of these manipulation experiments were performed by using the “lateral manipulation” mode to reposition an atom or molecule on a surface by moving the particle laterally without it leaving the surface. This often requires a smooth surface with small surface potential energy corrugations, such as low Miller index metal surfaces, and it works well at low temperatures to hinder the random motion of the manipulated atoms.<sup>14</sup> However, atomic manipulation at room temperature is of great practical importance for fabricating nanodevices and for the studies related to chemical activities and catalysis. Several successful room temperature manipulations have been demonstrated, including the lateral moving of Br atoms across Cu(100),<sup>16</sup> desorbing,<sup>17</sup> and dissociating<sup>18</sup> single chlorobenzene molecules from Si(111). More recently, the AFM cantilever was used to manipulate native atoms on an Si(111)-(7×7) surface at room temperature *via* atomic vacancy,<sup>19</sup> and even to demonstrate a reversible vertical concerted exchange of Si–Sn atoms between the Si AFM cantilever and the Sn atoms deposited on an Si(111) surface.<sup>20</sup> Yet, none of the above experiments

\* Address correspondence to xdxiao@phy.cuhk.edu.hk.

Received for review July 14, 2011 and accepted August 6, 2011.

Published online August 07, 2011  
10.1021/nn202636g

© 2011 American Chemical Society

succeeded in reversibly transferring atoms between the surface and the tip at designated positions at room temperature. On highly corrugated surfaces, such as Si(111)-(7×7), lateral manipulation of atoms is not possible because the surface potential is highly inhomogeneous and the energy barriers are too high to cross. Therefore, to manipulate an atom from one position to another, one has to rely on the “vertical manipulation” mode, in which an atom/molecule is transferred to the scanning probe of STM/AFM and then transferred back to the surface at the designated position in a controlled manner.<sup>14,15,21</sup> Because stringent conditions are required for the transfer and reverse transfer of the particles,<sup>15</sup> only a few reversible vertical manipulations have hitherto been demonstrated by applying an appropriate bias voltage. Reproducible examples include Xe atoms on Ni(110)<sup>21</sup> and CO on Cu(111).<sup>22</sup> The challenge for manipulating a metal atom in the vertical manipulation mode is that, to reversibly transfer the atom between the STM tip and the surface, it is necessary to overcome a much stronger potential barrier compared to that for a weakly bonded *gas* atom on a metallic surface. On semiconductor and oxide surfaces, atom/molecules often adsorb *via* a covalent bond that makes vertical manipulation more difficult.

In this paper, we report successful experiments to perform reproducible and reversible vertical manipulation by STM at room temperature. Single Ag atoms adsorbed on a Si(111)-(7×7) surface are transferred to the STM tip and then dropped off by following designated procedures. This technique is observed to be reliable and can be applied to manipulate the Ag atoms to form complex Ag structures. The Si(111)-(7×7) reconstruction surface has a large unit cell (~2.7 nm), which consists of a faulted half unit cell (FHUC) and an unfaulted half unit cell (UHUC). These half unit cells (HUCs) trap Ag atoms by much higher inter-HUC barriers and form a template for the formation of Ag clusters.<sup>23–25</sup> Through adding or removing Ag atoms one by one to (or from) a designated HUC, we have demonstrated the assembling and disassembling of large Ag nanostructures. The precise control of single Ag atoms enables us to determine that the maximum occupation in a HUC is 25 Ag atoms.

## RESULTS AND DISCUSSION

After the deposition of a small amount of Ag atoms, most of the Ag atoms are trapped within the HUCs and form Ag<sub>1</sub> (Ag monomer) and Ag<sub>2</sub> (Ag dimer) structures.<sup>23,24</sup> The Ag atoms are diffusing fast inside the HUCs at room temperature, whereas their inter-HUC diffusion is much suppressed.<sup>23,26,27</sup> In this paper, a structure containing *n* Ag atoms is denoted by Ag<sub>*n*</sub>. Although these Ag structures do not show any change during normal STM imaging, we found that the Ag atoms in these structures can be transferred to the STM

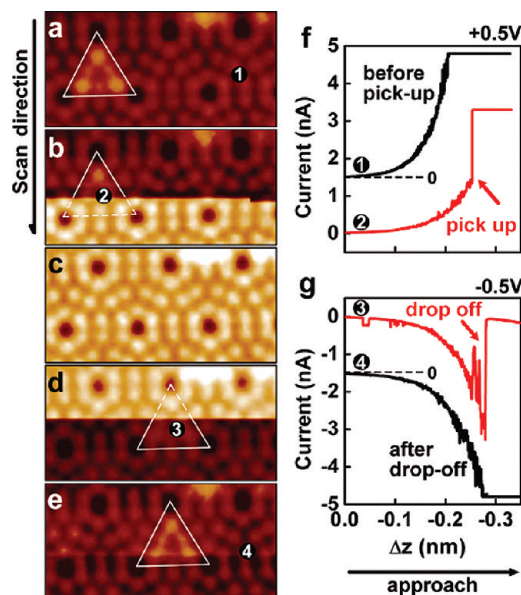


**Figure 1.** (a–e) A series of STM images (8.6 nm × 4.9 nm) showing the basic procedures of the vertical transfer of a single Ag atom on an Si(111)-(7×7) surface to the STM tip and *vice versa*. (a) An Ag<sub>1</sub> structure appears in the area of a FHUC which is marked by a triangle. The Ag atom is picked up by the STM tip in panel b and is dropped off to another FHUC in panel d. The adsorption of the Ag atom at the tip apex induces a higher brightness of the STM image in panel c and in part of panels b and d. (f) Tunneling current *versus* tip displacement during the approach of the STM tip at +0.5 V sample bias (pick-up procedure). The positions are marked in panel a for the line “before pick-up” and in panel b for the line “pick-up”. (g) Tunneling current *versus* tip displacement during approaching the STM tip at -0.5 V sample bias (drop-off procedure). The positions are marked in panel d for the line “drop-off” and in panel e for the line “after drop-off”. An arrow is used to indicate a sudden current change in panels f and g. The flat part in the curve “before pick-up” and “pick-up” in panel f and “after drop off” in panel g is caused by the current limitations of our instrument.

tip apex and *vice versa* through the appropriate procedures. Figure 1 shows an example of picking up and dropping off an Ag atom. In Figure 1a, a triangle highlights an Ag<sub>1</sub> structure in a FHUC, whereas the other HUCs are empty. The triangle morphology of Ag<sub>1</sub> is resulted from the hopping of the Ag atom within the FHUC at a much faster rate than the scanning speed of the STM tip, and thus represents its characteristic time averaged STM image.<sup>26</sup> Figure 1b shows the next STM image which appears the same as in Figure 1a in the upper part (the scanning direction is from top to bottom), until the imaging process is interrupted by a pick-up procedure inside the HUC of the Ag<sub>1</sub> structure (the position is marked by a round spot). With the Ag atom transferred to the tip apex, the STM tip becomes longer. This, in turn, makes the STM topography become higher by about 1.2 Å, as is shown by the brighter contrast in the lower part of the STM image in Figure 1b. The lattice of the Si(111)-(7×7) surface also shows a lateral shift of ~1 Å which is attributed to the laterally shifted tip apex by the Ag atom. The adsorption

of the Ag atom at the STM tip causes a sudden increase of the recorded tunneling current during the approach of the STM tip, as is shown by the line “pick-up” in Figure 1f. In contrast, the line “before pick-up” shows an exponentially increased current when the pick-up procedure is conducted at a position without any Ag structures (as marked by a round spot in Figure 1a), where no atom transfer happens. This indicates that the atom transfer can only be achieved in the area underneath the very tip of the apex.

The STM tip with the extra Ag atom cannot pick up another Ag atom from the surface but it can still produce stable and high-resolution STM images. Figure 1c shows the STM image in which the Ag1 structure in Figure 1a has disappeared from the surface. In Figure 1d, the Ag atom is dropped off from the tip to another FHUC at a position inside the target FHUC (as marked by a round spot) by using the drop-off procedure. As a reverse process of the Ag atom pick-up in Figure 1b, the image brightness and the lateral shift change back to the situation before picking up the Ag atom in Figure 1b. Moreover, the tunneling current during approaching the tip (the line “drop-off” in Figure 1g) shows a sudden decrease because the STM tip becomes shorter. A close examination on the noisy tunneling current signals in Figure 1g before the line “drop-off” also demonstrates that the Ag atom on the tip is not stationary, possibly moving back-and-forth between the tip and the surface before the Ag atom finally jumped to the surface. Figure 1e shows a complete image of the Ag1 structure in the target FHUC. A further trial of the drop-off procedure (the position is marked by a round spot in Figure 1e) produces no change on the surface, and the tunneling current shows an exponential increase as the tip gets closer to the surface, as is shown by the line “after drop-off” in Figure 1g.

Our results show that only one Ag atom can be picked up by the STM tip at a time. Similarly, only the picked Ag atom can be dropped off from the tip. In our experiments, the success rate of the pick-up or drop-off event is higher than 90%. Even if the tip failed to pick up or drop off an Ag atom, the conditions of the tip and the surface will usually remain unchanged and no damage will happen to the surface from applying the pick-up or drop-off procedures. No obvious tip position dependence inside the HUC is observed for picking up or dropping off a Ag atom, possibly because the Ag atom is diffusing fast within the HUC. Furthermore, the transfer of the Ag atoms is always accompanied with a reversible tip height change and a tunneling current change, leading to an easy judgment on the success of the Ag atom transfer. Whereas the characteristics of these changes vary depending on the tip conditions, the used parameters for pick-up/drop-off procedures, including the tip approaching distance to the sample surface ( $\sim 3.5$  Å) and the sample bias (+0.5 V/−0.5 V)

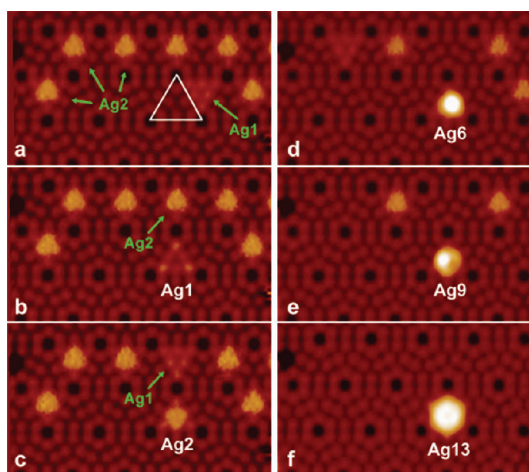


**Figure 2.** A series of STM images ( $13.4 \text{ nm} \times 8.1 \text{ nm}$ ) of an Si(111)-(7 $\times$ 7) surface showing the processes of the assembling of Ag nanostructures in a FHUC by adding Ag atoms one-by-one. An Si defect at the left edge of each of these images marks the same area. In panel a, one Ag1 structure and six Ag2 structures appear on the surface, all in UHUCs. In panel a, a triangle marks the empty target FHUC for the assembling. Panels b, c, d, e, and f show, respectively, constructed structures of Ag1, Ag2, Ag6, Ag9, and Ag13.

during atom transfer, have been optimized for the best success rate and reliability.

The capability of this technique is far more than the basic atom transportation demonstrated above. We find that the pick-up and drop-off procedures are also effective in constructing complex Ag structures. Figure 2 shows six STM images during the assembly of an Ag13 cluster by transporting 13 Ag atoms one-by-one to a FHUC. In Figure 2a, there are six Ag2 structures and one Ag1 structure all in the UHUCs. A triangle marks a FHUC as the targeted position for assembling an Ag cluster. First, the Ag atom in the Ag1 structure in Figure 1a is picked up by the STM tip and dropped off to the target FHUC. In Figure 2b, the next STM image shows an Ag1 structure in the target FHUC while the Ag1 structure marked in Figure 1a has been removed. Second, another Ag atom is picked up from an Ag2 structure (marked by an arrow in Figure 2b) and is dropped off to the target FHUC. In Figure 2c, the target FHUC shows an Ag2 structure while the marked Ag2 structure in Figure 2b loses one Ag atom and becomes an Ag1 structure. By continuously picking up Ag atoms from the surrounding UHUCs and dropping them off to the target FHUC, the Ag3–Ag13 structure can be assembled in the target FHUC. Figure 2 panels d–f show a selection of STM images showing Ag6, Ag9, and Ag13 structures in the target FHUC. In each of these STM images in Figure 2, 13 Ag atoms appear in the same area. After the formation of Ag1 in the target FHUC, the following drop-off processes are essentially conducted above the existing Ag structures, for example, Ag1–Ag12, and all the drop-off events are effective. All the structures fabricated in the target FHUC, from Ag1 to Ag13, show exactly the same STM image

as those grown by Ag thermal growth.<sup>23</sup> This indicates that these manipulations do not perturb the formation of Ag structures in the FHUC.

In our previous work, the number of atoms in structures with more than 13 Ag atoms thermally grown on HUCs cannot be identified because of the disturbance of other Ag structures in the surrounding areas.<sup>23</sup> With the atom manipulation capability, we can now build even larger isolated Ag structures and obtain direct information on them. By using the same method described in Figure 2, up to 25 Ag atoms could be assembled and stably located inside a FHUC. To demonstrate the growth process of the Ag structures more clearly, we assembled Ag1 to Ag25 in 25 FHUCs in the same STM image and arranged them in a  $5 \times 5$  array, as shown in Figure 3a. Here, a total of 325 Ag atoms are manipulated to designated positions for this result. For most of these Ag structures, the images are stable. However, for Ag1 and Ag2, the Ag atoms are moving fast within the HUC. For Ag7, we have still seen hopping features in Figure 3a, whereas in other images of the same area it can be clearly imaged without such hopping features.<sup>23</sup> For a comparison, Figure 3b shows the STM images of Ag1–Ag13 which is formed naturally when the Ag coverage is much larger, for example, 0.06 ML. Their numbers of atoms contained in these clusters are determined by continuous observation of the diffusion of single Ag atoms among HUCs which causes the association or disassociation of the Ag clusters.<sup>23</sup>

Because all of the HUCs on the Si-(7 $\times$ 7) substrate have a 3-fold symmetry, the Ag structures in Figure 3a should be rotated to the equivalent orientations for comparison. Thus, a general picture of the growth process from Ag1 to Ag25 can be clearly identified: the Ag atoms of Ag1 and Ag2 diffuse fast inside a FHUC and result in time-averaged STM images. From Ag3 onward, the Ag atoms practically stop diffusing and form cluster-like structures shown as the bright images. The size of the bright area gradually increases in the inner part of the FHUC until Ag9. Ag10 to Ag13 show rounded plate morphology and their apparent sizes increase monotonically from the center of the FHUC. For Ag14, a sudden change occurs and the image becomes bright only at one of the three corners of the FHUC. This indicates that the Ag atoms start to occupy the sites near the corner of the FHUC. From Ag14 to Ag17, the images increase their size and brightness mainly at the center part of the FHUC. At Ag18, two corners of the FHUC start to become bright and the third corner of the FHUC remains very dim, indicating that Ag atoms occupy the sites near the second corner of the FHUC. The following growth process up to Ag23 is again at the center part, and it is similar to that after Ag14. At Ag23, the sites near the third corner start to be occupied, with Ag24 and Ag25 becoming more completely occupied in the FHUC to

reach a 3-fold symmetry. The structures Ag23 to Ag 25 look quite similar, with a minute difference in the brightness of the corners.

The STM images and the known number of atoms can provide clues to the atomic configurations of these Ag structures. In Figure 3a, we also depict plausible models of the configurations for these Ag structures next to their STM images. It is known that a single Ag atom prefers high coordination sites as the adsorption sites in a HUC.<sup>26,28</sup> We simply follow this rule to place Ag atoms onto these sites surrounded by the Si rest atoms and Si adatoms of the FHUC. The STM image of Ag1 structure showing a bright triangle resulted from the fast diffusion of the Ag atom among different adsorption sites. The image of the Ag2 structure is also affected by the fast motion of the Ag atoms. At low temperature, the Ag1 in FHUC was observed adsorbing at the high coordination sites near the corner Si adatoms,<sup>26</sup> and the Ag2 was observed to adsorb at the two high coordination sites near one of the center Si adatoms.<sup>29</sup> The very center site of the FHUC is only a local energy minimum for a single Ag atom.<sup>26</sup> However, with two other Ag atoms adsorbed at the two high coordination sites next to the center Si adatom, the third Ag atom can adsorb at the very center site of the FHUC to form a trimer of Ag3 through the interaction with the two high-coordination Ag atoms, as demonstrated by first-principles calculations.<sup>29</sup> From Ag4 to Ag10, the additional Ag atoms continue to adsorb at the other high coordination sites in the inner parts of a FHUC. Afterward, for example, for Ag11–Ag13, new Ag atoms start to occupy the center sites at the edges of the FHUC. These outer Ag atoms segregate to corner sites and form a bright feature for Ag14. Then, the edge sites are occupied one-by-one to increase the size of the Ag structure, until the sites near the second corner start to be occupied for Ag18 and the sites near the third corner start to be occupied for Ag23, respectively. Finally, at Ag25 all the possible high coordinate sites inside the FHUC are occupied. The resulting atomic configuration model corresponds well to the STM image of Ag25, showing a very symmetric triangular pattern. We must note that the adsorption sites at the edges are not calculated, rather they are from the consideration of systematic filling of the Ag atoms within the FHUC, possibly required by the interaction with the existing Ag atoms in the Ag structures. The validity of the atomic configuration for the structures above Ag10 needs to be confirmed by future theoretical calculations.

The FHUC could stably accommodate as many as 25 Ag atoms in one layer, as shown in the zooming image of the Ag25 structure shown in Figure 4a. Transferring one additional Ag atom to the Ag25 structure will induce an unstable Ag26 structure (Figure 4b). The Ag26 structure shows bright fuzzy features in the FHUC and the surrounding three UHUCs. This implies that the



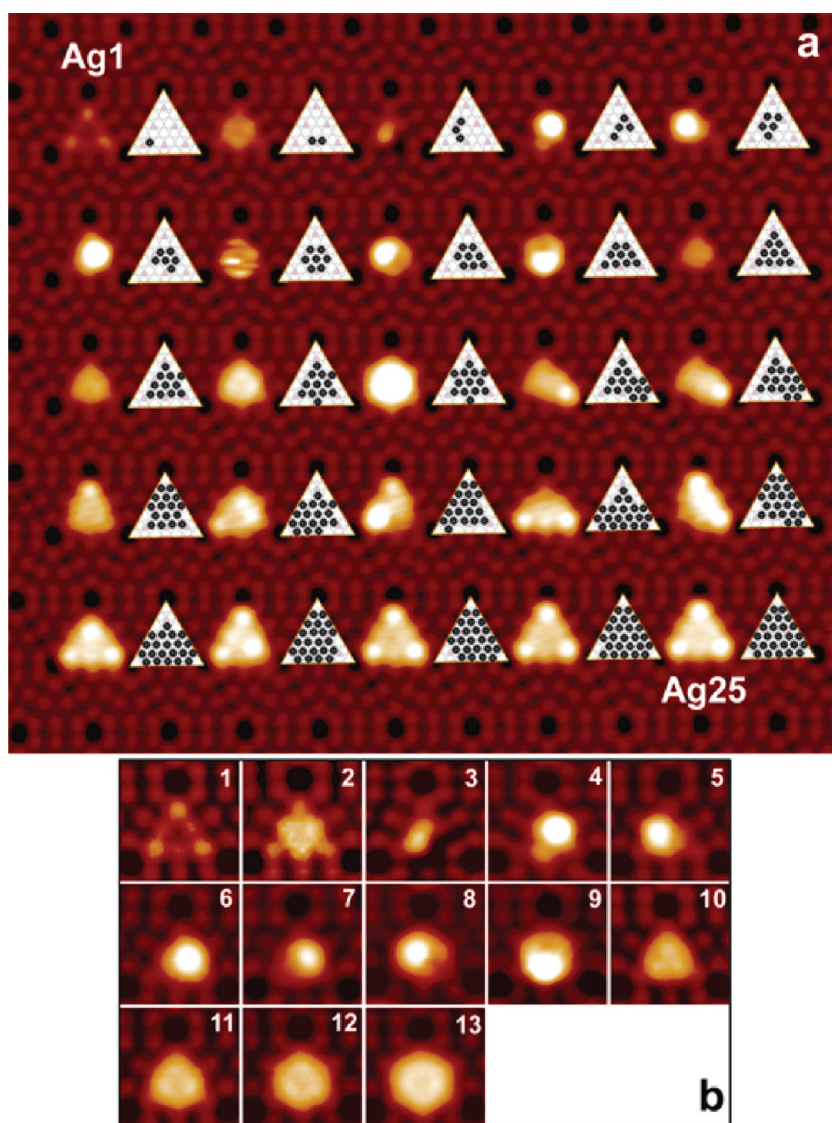


**Figure 3.** (a) An STM image ( $28.2 \text{ nm} \times 25.6 \text{ nm}$ ) showing 25 Ag structures, Ag1–Ag25, sequentially arrayed in five rows. At the right side of each structure, a plausible structural model is proposed by showing the lateral positions of the Ag atoms. (b) STM images showing the Ag1–Ag13 grown by thermal process.

additional Ag atom is hopping between the four HUCs with a rate similar to the scanning line speed of the STM tip and it does not stay on the top of the first Ag layer. Structure Ag27 also shows a fuzzy feature with hopping of more Ag atoms in the four HUCs (Figure 4c). When a total of 28 Ag atoms are assembled, the additional Ag atoms seem to gather into one instead of three neighboring UHUCs and show a protrusion in only one UHUC (STM image not shown here). When more Ag atoms are added to the structure, the protrusion grows and gradually occupies the UHUC. However, probably because of the interaction of Ag structures in the neighboring HUCs, the Ag25 structure in FHUC could hardly maintain its original morphology after the Ag atom spill-off to a neighboring UHUC. Figure 4d shows the Ag50 structure which occupies almost a full unit cell of Si(111)-(7 $\times$ 7). Another spill-off happens and a new protrusion starts to grow in the

second FHUC when there about 55 Ag atoms. Figure 4e shows the STM image of the Ag62 structure that occupies three HUCs with the arrow indicating the new protrusion in the second FHUC. The fuzzy feature shows the hopping of Ag atoms on top of the Ag62 structure. As seen from the line profiles in Figure 4f, a second layer of Ag atoms starts to form which appears to be about 2 Å higher than the Ag25 structure below.<sup>30,31</sup>

Unlike what occurred in FHUC, in which Ag25 is a stable structure and may be described by the configuration in Figure 3a, we find it impossible to assemble an isolated Ag structure in UHUC with more than 13 Ag atoms. Adding an extra Ag atom into Ag13 in an UHUC makes the new structure very unstable, and several Ag atoms will diffuse into one of neighboring FHUCs and they will function as a seed for further growth. This may also explain that even next to an Ag25 in a FHUC, the

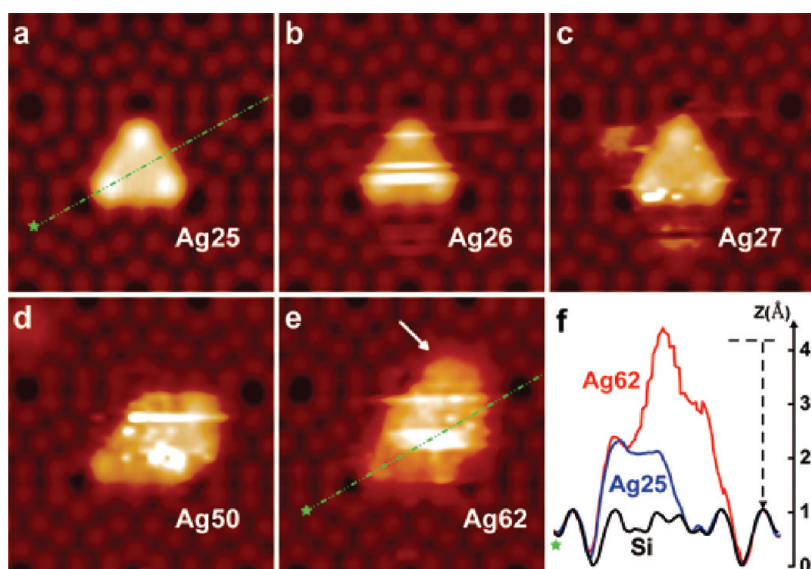


**Figure 4.** (a–e) The STM images ( $6.7 \text{ nm} \times 7.0 \text{ nm}$ ) of Ag<sub>25</sub>, 26, 27, 50, and 62 assembled by manipulation. (f) Line profiles of Ag structures and Si. The positions for Ag<sub>25</sub> and Ag<sub>62</sub> are indicated in panels b and f. The dashed line and arrow show the height of a one-layer step of an Si(111)-(7 $\times$ 7) surface.

stability of an assembled Ag structure in the UHUC is weaker and no perfect Ag<sub>50</sub> structure can be assembled.

The Ag clusters can also be disassembled by removing Ag atoms out of the structure in a one-by-one atom fashion, indicating that the pick-up procedure is effective not only for simple Ag structures but also for complex Ag structures. Figure 5a shows an STM image of an Ag<sub>25</sub> structure in FHUC assembled previously whereas the surrounding HUCs are all empty except for a mark on the top part of the image. The Ag atoms are picked up by the STM tip from the FHUC of the Ag<sub>25</sub> structure and each of these Ag atoms is dropped off to the surrounding empty FHUCs one-by-one until the FHUC of the Ag<sub>25</sub> becomes empty. In Figure 5b, the triangle marks the empty FHUC (the one in which the Ag<sub>25</sub> was situated) and it shows that the Si(111)-(7 $\times$ 7) structure is preserved. However, only 23 Ag atoms are removed from the Ag<sub>25</sub> structure, as is shown by the 23 Ag<sub>1</sub> structures in Figure 5b. Two movies showing the assembling and disassembling of an Ag<sub>25</sub> structure are available in the Supporting Information. During the disassembling process the Ag structures sometimes exhibit unusual structures that show configurations which are different from those produced during the assembling process. One possible reason for this is that the disassembling process may produce other stable or substable structures which could hardly exist during the assembling process. Another reason is that the adsorption of Ag atoms at the corner holes (which is described below), may affect the structure inside the FHUC.

The two “missing” Ag atoms are lost to the corner hole sites of the FHUC, as marked by the triangle in Figure 5b. In Figure 6, we compare the line profiles

through the corner holes to show when the adsorption of the Ag atoms takes place during the course of disassembling the Ag<sub>25</sub> structure. The STM image in Figure 6a shows part of the area of Figure 5a after 20 Ag atoms have been removed out of the Ag<sub>25</sub> structure. The three corner holes of the FHUC are labeled by “A”, “B”, and “C”, respectively. The line profiles corresponding to Figure 6a indicate that the corner hole A appears to be shallower than corner hole B and C, which appear to be the same height as the other corner holes away from this FHUC. This demonstrates that one Ag atom is now adsorbed at the corner hole site A while the two other corner hole sites are empty. After one more Ag atom is picked up from the target FHUC, the STM image (Figure 6b) shows an Ag<sub>2</sub> structure in the FHUC. The line profiles in Figure 6b show that the corner hole C now becomes shallower by  $\sim 0.23 \text{ \AA}$ , similar to corner hole A, and this implies that another Ag atom has been adsorbed at the corner hole site C. The heights of these corner holes stays unchanged after moving the remaining two Ag atoms out of the FHUC, as is shown in Figure 6b. Therefore, we identified that the two missing Ag atoms are unambiguously adsorbed at the two corner hole sites and that the total number of the Ag atoms, as shown in Figure 5b, is conserved to 25 Ag atoms. The corner hole site A is observed to gain the Ag atom (STM image not shown here) after nine Ag atoms have been moved out of the Ag<sub>25</sub> structure, as shown in Figure 5a.

The adsorption of Ag atoms at corner hole sites is also observed with a small dose of Ag atoms by examining the line profiles in their STM images. Calculations show high barriers around the corner holes,<sup>26</sup> which may forbid the diffusion of Ag atoms from inside the HUC to the holes. In our STM imaging, no diffusion

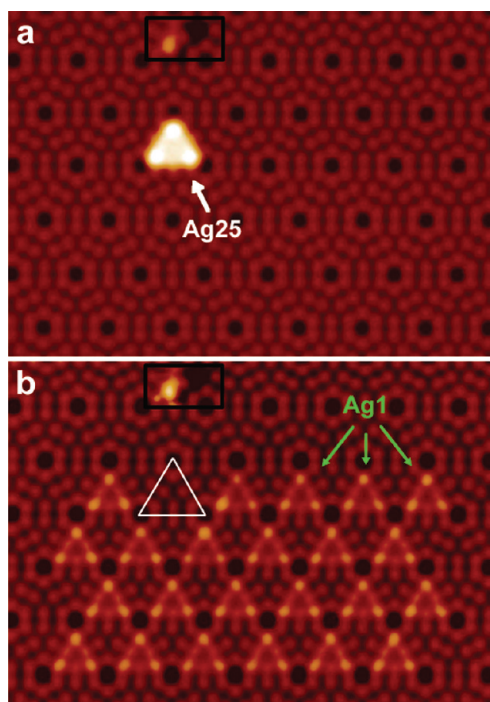


**Figure 5.** (a) An STM image ( $20.2 \text{ nm} \times 13.2 \text{ nm}$ ) showing a Ag25 structure in a FHUC of an Si(111)-(7 $\times$ 7) surface. An Si defect indicated by a square box above the Ag25 structure marks the position of the area. (b) An STM image of the same area as panel a, showing 23 Ag1 structures arrayed on the surface after the disassembling of the Ag25 structure in panel a. A triangle in panel b marks the empty FHUC where the Ag25 locates in panel a.

event is observed between the other Ag adsorption sites and a corner hole site. Without examining the depth of the corner holes, the atom in a corner hole can be hardly observed from the STM images because with or without the Ag atom in the corner hole the image always appears dark. To our knowledge, this is the first experimental demonstration of the adsorption of a single metal atom at the corner hole site. Previous works on the Ag nanostructures or Ag growth on an Si(111)-(7 $\times$ 7) surface have not paid enough attention to the corner holes sites.<sup>23–25</sup> Further work is required to explore the nature and the behavior of the corner hole Ag atoms.

The success of our reversible and reproducible manipulation of Ag atoms critically depends on the condition of the tip apex. A manipulation-functional tip should have a stable adsorption site whose adsorption energy is similar to that of the sites on the Si(111)-(7 $\times$ 7) surface. It is most probably that such function is determined by the local atomic and electronic structure rather than the material of the STM tip. In our experiments, making a manipulation-functional tip is a trial and error process with continuous modifying the tip apex by applying voltage pulses until it works. Besides Ag, the same method works well for Au atoms in assembling or disassembling Au clusters on the Si(111)-(7 $\times$ 7) surface, as already demonstrated in our

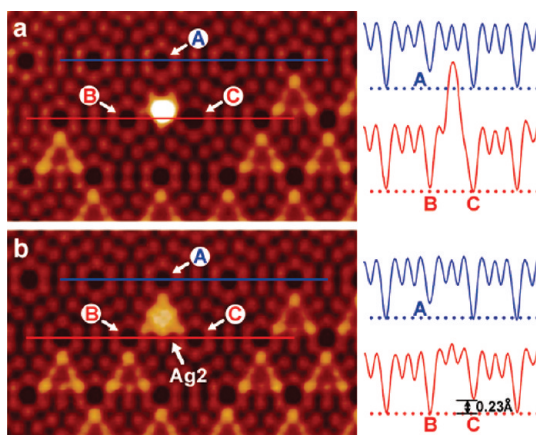


**Figure 6.** (a,b) Two STM images and their line profiles showing the change of depth of the corner holes after moving 20 (a) and 21 (b) Ag atoms out of an Ag25 structure described in Figure 5.

lab. The similar electronic structures of noble metal atoms imply this technique may also work for Cu atoms. However, the applicability to other elements on Si(111)-(7 $\times$ 7) or on other surfaces remains to be tested in future work.

## CONCLUSIONS

In summary, we have demonstrated that single Ag atoms adsorbed in HUCs of a Si(111)-(7 $\times$ 7) surface could be reversibly transferred to an STM tip and back to the surface. The transfer of the Ag atoms causes a sudden change of the tunneling current as well as a change in the STM image. This technique is reliable and reproducible. Transferring a number of Ag atoms to a single HUC allows us to construct complex Ag clusters which could hardly be obtainable by natural Ag growth. The maximum number of Ag atoms in an HUC is determined to be 25 and assembling more Ag atoms will cause a spill-off of an Ag atom into neighboring HUCs. This corresponds well with our atomic model which shows that the Ag atoms could stably accommodate at the high coordination sites and form a planar structure. We have also demonstrated the disassembling of an Ag25 cluster into single Ag atoms. In the course of the disassembling, the corner hole sites of an Si(111)-(7 $\times$ 7) surface are observed to adsorb single Ag atoms which reduces the depth of the corner holes in the STM images. This reliable vertical manipulation of the Ag atoms is expected to be applicable in constructing other nanoclusters and even nanodevices on an Si(111)-(7 $\times$ 7) surface. With the atomic manipulation technique at ambient temperature being developed as a tool to study clusters, we believe it would open up new perspectives in the hot topics of nanoscience, for example building clusters to study their electronic or spin behaviors; modifying the catalytic active sites of nanoparticles; fabricating ultrasmall nanoelectrodes and nanodevices at ambient temperatures; and tuning plasmonic characteristics of



nanoparticles by changing the atomic structures. The full potential of the atomic manipulation as a common

experimental tool is enormous and yet awaits to be further revealed.

## EXPERIMENTAL METHODS

Our experiments were carried out with an Omicron variable temperature STM, which is operated in an ultrahigh vacuum with a base pressure  $<1 \times 10^{-10}$  Torr. A n-type Si(111) wafer with a room temperature resistivity of  $\sim 0.026 \Omega \cdot \text{cm}$  was used as the substrate. It is first degassed at  $\sim 900$  K for several hours in the ultrahigh vacuum environment until the base pressure is better than  $5 \times 10^{-10}$  Torr. Then the wafer is flash annealed to  $\sim 1500$  K for several times and afterward cooled down slowly from 1200 K to room temperature to form a well reconstructed Si(111)-(7 $\times$ 7) surface. A Mo crucible with Ag source is heated by electron beam and about  $3 \times 10^{-3}$  monolayer (1 monolayer =  $1.38 \times 10^{15}$  atoms/cm<sup>2</sup>) Ag was deposited onto the Si(111)-(7 $\times$ 7) surface which is kept at room temperature. A tungsten tip was used for the STM imaging and the images were taken at a sample bias of +2 V and a tunneling current 0.01 nA at room temperature. The vertical atomic manipulation consists of three stages: atom pick-up, translation, and atom drop-off. In the atom pick-up stage, an Ag atom can be transferred from the surface to the tip apex by the following procedure: first, position the STM tip above a Ag structure at the STM set-point conditions (+2 V, 0.01 nA); second, switch the sample bias to +0.5 V and then disable the feedback loop; and, third, approach the tip to the surface for about 3.5 Å. The transfer of an Ag atom to the STM tip will likely occur and can be reflected by the monitored tunneling current. Finally, retract the tip, resume the feedback, and set back the bias voltage to +2 V. The drop-off stage, that is, the transfer of an Ag atom from the STM tip back to the surface, takes a similar procedure but one which uses an applied sample bias of -0.5 V during the tip approaching process. The translation stage is accomplished by moving the STM tip with the picked Ag atom at the normal scanning set-point conditions.

**Acknowledgment.** This work was supported by the Research Grants Council of Hong Kong (N\_CUHK616/06) and the Natural Science Foundation of China (50618001).

**Supporting Information Available:** Two movies showing the assembling and disassembling of an Ag<sub>25</sub> cluster. This material is available free of charge via the Internet at <http://pubs.acs.org>.

## REFERENCES AND NOTES

- Haberland, H.; Hippler, T.; Donges, J.; Kostko, O.; Schmidt, M.; von Issendorff, B. Melting of Sodium Clusters: Where Do the Magic Numbers Come from? *Phys Rev. Lett.* **2005**, *94*, 035701.
- Creyghton, E. J. Zeolites: Organic Groups Cling to the Pores. *Nature* **1998**, *393*, 21–22.
- Moro, R.; Xu, X.; Yin, S.; de Heer, W. A. Ferroelectricity in Free Niobium Clusters. *Science* **2003**, *300*, 1265–1269.
- Haruta, M. Size- and Support-Dependency in the Catalysis of Gold. *Catal. Today* **1997**, *36*, 153–166.
- Bamwenda, G. R.; Tsubota, S.; Nakamura, T.; Haruta, M. The Influence of the Preparation Methods on the Catalytic Activity of Platinum and Gold Supported on TiO<sub>2</sub> for CO Oxidation. *Catal. Lett.* **1997**, *44*, 83–87.
- Valden, M.; Lai, X.; Goodman, D. W. Onset of Catalytic Activity of Gold Clusters on Titania with the Appearance of Nonmetallic Properties. *Science* **1998**, *281*, 1647–1650.
- Roach, P. J.; Woodward, W. H.; Castleman, A. W.; Reber, A. C.; Khanna, S. N. Complementary Active Sites Cause Size-Selective Reactivity of Aluminum Cluster Anions with Water. *Science* **2009**, *323*, 492–495.
- Li, J.; Li, X.; Zhai, H.-J.; Wang, L.-S. Au<sub>20</sub>: A Tetrahedral Cluster. *Science* **2003**, *299*, 864–867.
- Gruene, P.; Rayner, D. M.; Redlich, B.; van der Meer, A. F. G.; Lyon, J. T.; Meijer, G.; Fielicke, A. Structures of Neutral Au<sub>7</sub>, Au<sub>19</sub>, and Au<sub>20</sub> Clusters in the Gas Phase. *Science* **2008**, *321*, 674–676.
- Eigler, D. M.; Schweizer, E. K. Positioning Single Atoms with a Scanning Tunneling Microscope. *Nature* **1990**, *344*, 524–526.
- Heinrich, A. J.; Lutz, C. P.; Gupta, J. A.; Eigler, D. M. Molecule Cascades. *Science* **2002**, *298*, 1381–1387.
- Bartels, L.; Meyer, G.; Rieder, K. H. Basic Steps of Lateral Manipulation of Single Atoms and Diatomic Clusters with a Scanning Tunneling Microscope Tip. *Phys. Rev. Lett.* **1997**, *79*, 697.
- Stroscio, J. A.; Eigler, D. M. Atomic and Molecular Manipulation with the Scanning Tunneling Microscope. *Science* **1991**, *254*, 1319–1326.
- Hla, S. W. Scanning Tunneling Microscopy Single Atom/Molecule Manipulation and Its Application to Nanoscience and Technology. *J. Vac. Sci. Technol., B* **2005**, *23*, 1351–1360.
- Gauthier, S. Atomic and Molecular Manipulations of Individual Adsorbates by STM. *Appl. Surf. Sci.* **2000**, *164*, 84–90.
- Fishlock, T. W.; Oral, A.; Egde, R. G.; Pethica, J. B. Manipulation of Atoms Across a Surface at Room Temperature. *Nature* **2000**, *404*, 743–745.
- Sloan, P. A.; Hedouin, M. F. G.; Palmer, R. E.; Persson, M. Mechanisms of Molecular Manipulation with the Scanning Tunneling Microscope at Room Temperature: Chlorobenzene/Si(111)-(7 $\times$ 7). *Phys. Rev. Lett.* **2003**, *91*, 118301.
- Sloan, P. A.; Palmer, R. E. Two-Electron Dissociation of Single Molecules by Atomic Manipulation at Room Temperature. *Nature* **2005**, *434*, 367–371.
- Sugimoto, Y.; Jelinek, P.; Pou, P.; Abe, M.; Morita, S.; Perez, R.; Custance, O. Mechanism for Room-Temperature Single-Atom Lateral Manipulations on Semiconductors Using Dynamic Force Microscopy. *Phys. Rev. Lett.* **2007**, *98*, 106104.
- Sugimoto, Y.; Pou, P.; Custance, O.; Jelinek, P.; Abe, M.; Perez, R.; Morita, S. Complex Patterning by Vertical Interchange Atom Manipulation Using Atomic Force Microscopy. *Science* **2008**, *322*, 413–417.
- Eigler, D. M.; Lutz, C. P.; Rudge, W. E. An Atomic Switch Realized with the Scanning Tunneling Microscope. *Nature* **1991**, *352*, 600–603.
- Bartels, L.; Meyer, G.; Rieder, K. H. Controlled Vertical Manipulation of Single CO Molecules with the Scanning Tunneling Microscope: A Route to Chemical Contrast. *Appl. Phys. Lett.* **1997**, *71*, 213–215.
- Ming, F.; Wang, K.; Zhang, X.; Liu, J.; Zhao, A.; Yang, J.; Xiao, X. Identifying the Numbers of Ag Atoms in Their Nanostructures Grown on a Si(111)-(7 $\times$ 7) Surface. *J. Phys. Chem. C* **2011**, *115*, 3847–3853.
- Ost'ádal, I.; Kocán, P.; Sobotík, P.; Pudl, J. Direct Observation of Long-Range Assisted Formation of Ag Clusters on Si(111) 7 $\times$ 7. *Phys. Rev. Lett.* **2005**, *95*, 146101.
- Tosch, S.; Neddermeyer, H. Initial Stage of Ag Condensation on Si(111) 7 $\times$ 7. *Phys. Rev. Lett.* **1988**, *61*, 349.
- Wang, K.; Chen, G.; Zhang, C.; Loy, M. M. T.; Xiao, X. Intermixing of Intra-basin and Inter-basin Diffusion of a Single Ag Atom on Si(111)-(7 $\times$ 7). *Phys. Rev. Lett.* **2008**, *101*, 266107.
- Sobotík, P.; Kocán, P.; Ost'ádal, I. Direct Observation of Ag Intercell Hopping on the Si(111)-(7 $\times$ 7) Surface. *Surf. Sci.* **2003**, *537*, L442–L446.
- Zhang, C.; Chen, G.; Wang, K.; Yang, H.; Su, T.; Chan, C. T.; Loy, M. M. T.; Xiao, X. Experimental and Theoretical Investigation of Single Cu, Ag, and Au Atoms Adsorbed on Si(111)-(7 $\times$ 7). *Phys. Rev. Lett.* **2005**, *94*, 176104.
- Hu, S.; Zhao, A.; Kan, E.; Cui, X.; Zhang, X.; Ming, F.; Fu, Q.; Xiang, H.; Yang, J.; Xiao, X. Electrical Rectification by



- Selective Wave-Function Coupling in Small Ag Clusters on Si (111)-(7×7). *Phys. Rev. B* **2010**, *81*, 115458.
30. Sobotik, P.; Ost'adal, I.; Myslivecek, J.; Jarolimek, T.; Lavický, F. Transition from 2D to 3D Growth During Ag/Si(111)-(7×7) Heteroepitaxy. *Surf. Sci.* **2001**, *482*, 797–801.
  31. Gavioli, L.; Kimberlin, K. R.; Tringides, M. C.; Wendelken, J. F.; Zhang, Z. Novel Growth of Ag Islands on Si(111): Plateaus with a Singular Height. *Phys. Rev. Lett.* **1999**, *82*, 129.